



HAL
open science

Treatment of cauliflower processing wastewater by nanofiltration and reverse osmosis in view of recycling

Céline Garnier, Wafa Guiga, Marie-Laure Lameloise, Laure Degrand, Claire Fargues

► To cite this version:

Céline Garnier, Wafa Guiga, Marie-Laure Lameloise, Laure Degrand, Claire Fargues. Treatment of cauliflower processing wastewater by nanofiltration and reverse osmosis in view of recycling. *Journal of Food Engineering*, 2022, 317, pp.110863. 10.1016/j.jfoodeng.2021.110863 . hal-03415172

HAL Id: hal-03415172

<https://hal.science/hal-03415172v1>

Submitted on 5 Jan 2024

HAL is a multi-disciplinary open access archive for the deposit and dissemination of scientific research documents, whether they are published or not. The documents may come from teaching and research institutions in France or abroad, or from public or private research centers.

L'archive ouverte pluridisciplinaire **HAL**, est destinée au dépôt et à la diffusion de documents scientifiques de niveau recherche, publiés ou non, émanant des établissements d'enseignement et de recherche français ou étrangers, des laboratoires publics ou privés.



Distributed under a Creative Commons Attribution - NonCommercial 4.0 International License

Treatment of cauliflower processing wastewater by nanofiltration and reverse osmosis in view of recycling

Céline GARNIER¹, Wafa GUIGA^{1,2}, Marie-Laure LAMELOISE¹, Laure DEGRAND^{1,2} and Claire FARGUES^{1*}

¹Université Paris-Saclay, INRAE, AgroParisTech, UMR SayFood, 91300, Massy, France

²Conservatoire National des Arts et Métiers, UMR SayFood, 75003, Paris, France

*Corresponding author:

Claire Fargues, AgroParisTech, 1 avenue des Olympiades, 91744, Massy Cedex, France

claire.fargues@agroparistech.fr

Tel: +33 1 69 93 50 95

Declarations of interest : None.

Keywords

Membrane process, food industry, water reuse, effluent treatment, cauliflower, reverse osmosis

Abstract

The vegetable industry is a large consumer of drinking water. This paper investigates the possibilities of Reverse Osmosis (RO) or tight Nanofiltration (NF) for the treatment of cauliflower blanching wastewater with a view to recycling within the production unit. Ultrafiltration at 100 000 g.mol⁻¹ molecular weight cut-off was necessary to decrease turbidity below 1 NTU as required before NF or RO. Three NF (DK, NF270 and SRD3) and one RO (ESPA4) membranes were tested at bench-scale in a crossflow filtration mode. Only RO allowed to reach the desired quality for a reuse purpose, with an acceptable residual COD content of 225 mg O₂.L⁻¹. The Solution-Diffusion model was validated for the transfer of glucose and fructose, for NF270, DK and ESPA4 membranes and their permeability coefficients calculated.

Highlights:

- Ultrafiltration followed by reverse osmosis allows to consider recycling of cauliflower wastewater
- ESPA4 membrane at 19 bar leads to 70 L.h⁻¹.m⁻² permeate flux and 95% COD rejection
- Solution-diffusion model considering concentration polarization was successfully applied
- DK, NF270 and ESPA4 permeabilities for fructose and glucose were determined
- Nanofiltration with 150-300 g.mol⁻¹ molecular weight cut-off is not suitable, due to the transfer of small metabolites

34 1. Introduction

35 The industries that consume a large amount of water are more and more keenly concerned by the necessity to
36 save water resources. The food industry, including the fruit and vegetable transformation sector, is
37 particularly concerned: according to a study of the European Commission (European, 2018), water
38 consumption in the latter ranges from 0.5 to 15 m³/ton of processed raw material. Reuse (recycling without
39 treatment) and reconditioning (recycling after treatment) of these effluents thus become consequential in
40 order to reduce the environmental impact of these industries and restore water quality to an acceptable level.

41 Considered as robust, flexible and “green” (Dewettinck and Le, 2011; Guiga and Lameloise, 2019),
42 membrane processes are becoming favourite technologies for treating wastewater before recycling
43 (Warsinger et al., 2018; Wenten and Khoiruddin, 2016) especially for the food processing industry (Meneses
44 et al., 2017). Among them, reverse osmosis (RO) or tight nanofiltration (NF) ensure the highest water quality
45 and have already proved valuable for wastewater reconditioning in the dairy (Bortoluzzi et al., 2017; Brião et
46 al., 2019; Suárez et al., 2014) and brewery industries (Braeken et al., 2004). They can provide high permeate
47 fluxes and rejections at relatively low transmembrane pressure (*TMP*) provided several issues are considered:
48 first, adequate pre-treatment should be implemented to bring the Silt Density Index (SDI) to below 5 and
49 turbidity to 1 NTU (Sim et al., 2018). Second, membrane operations should be run below the critical flux to
50 avoid irreversible fouling (Aimar et al., 2010).

51 The possibilities of reuse and reconditioning of wastewater in the food industry, and the development of
52 toolboxes to evaluate the impact of these solutions are primary objectives in the French research program
53 MINIMEAU (ANR-17-CE10-0015). A recent study on carrot peeling wastewater highlighted that high-
54 quality water could be obtained through RO or tight NF membranes after microfiltration (MF) (Garnier et al.,
55 2020). In the vegetable-processing industry, one plant usually transforms different vegetables, either
56 simultaneously or successively. Consequently, the present study aimed to check the feasibility of the process
57 developed in Garnier et al. (2020) for wastewater arising from rinsing of carrots after peeling, for treating
58 wastewater from cauliflower blanching.

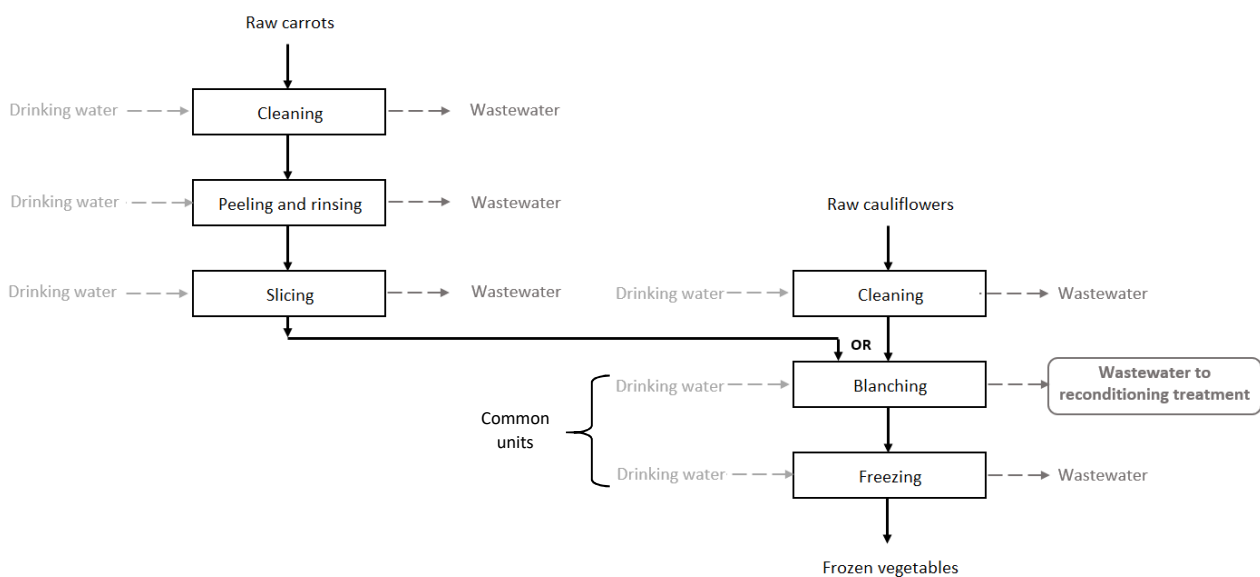
59 In the Drinking Water Standard, lists of parameters are to be respected for both drinking water quality and
60 the water source from which it originates (mainly surface or groundwater), while there is no regulatory
61 context outlining the water quality of recycled industrial wastewater. For food safety, drinking water is
62 usually requested in the food processing industry (Casani et al., 2005). In this work, characterisation of the
63 cauliflower blanching wastewater was made in order to select key parameters to be eliminated. Optimized
64 pre-treatment and membrane treatment were selected with drinking water quality as the objective. Finally,
65 the Solution-Diffusion model, commonly used to represent water and solutes transfer in non-porous
66 membranes (Qasim et al., 2019; Wijmans and Baker, 1995) was applied to obtain water and solutes
67 permeabilities for NF and RO membranes, considering the concentration polarization phenomenon. In this
68 work, it was acquired especially for sugars contained in cauliflower effluent, and compared with data

69 extracted from the literature results. Such database is essential for the design tool developed in the
70 MINIMEAU Project.

71 2. Material and Methods

72 2.1. Wastewater origins

73 The wastewater was obtained from the French factory already selected by the Technical Center for Food
74 Product Conservation (CTCPA, Paris, France) for the study of Garnier *et al.* (2020) on carrot processing
75 wastewater. This factory produces several frozen vegetables sometimes on the same production line.
76 Effluents of cauliflower processing are produced at the outlet of several operation units. In particular, a
77 cleaning unit is used only for cauliflower and a blanching and freezing unit alternately for all vegetables
78 (Fig. 1). Blanching consists in a short heat treatment with hot water (80 °C to 100 °C) to inactivate or delay
79 bacterial growth and enzyme action. Cauliflower wastewater collected at the outlet of the blanching
80 operation unit was selected for our study and stored at -18 °C before treatment tests. Drinking water used in
81 the factory was analysed as a reference.



82

83 **Fig. 1.** Schematic representation of vegetable processing operation in the factory under study.

84 2.2. Analytical methods

85 The following analyses were performed:

- 86 - Global parameters: Total Suspended Solids (TSS), particulate and dissolved Carbon Oxygen
87 Demand (COD), conductivity, pH, turbidity, Carbonate Hardness (CH), Total Nitrogen (TN), optical
88 density (OD), color,
- 89 - Dissolved organic pollution: glucose, fructose (accuracy $\pm 4\%$) and sucrose (accuracy $\pm 5\%$),

- 90 - Free and total chlorine (accuracy $\pm 0.06 \text{ mg.L}^{-1} \text{ Cl}_2$),
91 - Ionic composition: chloride, nitrite, nitrate, phosphate, sulphate, sodium, ammonium, potassium,
92 magnesium and calcium (accuracy $\pm 2.5\%$).

93 Most analytical methods are already described in Garnier *et al.* (2020). High-performance ion-exchange
94 chromatography (HPIC) was used to analyse anions and cations as well as sugars. At the pH of the effluent
95 (4.7) and based on the equilibrium diagram of CO_2 , the concentration of carbonate in the effluent was
96 negligible meaning that Carbonate Hardness (CH) could represent the concentration of bicarbonate.

97 COD (accuracy $\pm 3\%$), TN, CH (variable accuracy), chlorine (free and total) were determined with rapid test
98 tubes and photometric measurement (Nanocolor vis II - Macherey Nagel, Hoerdt, France). Color and
99 turbidity (accuracy $\pm 2\%$) were performed with the same photometric material. Color was established in the
100 CIELAB color space adopted by the International Commission on Illumination (CIE) in 1976, where color is
101 expressed as three values: L^* (lightness from black (0) to white (100)), a^* (from green to red) and b^* (from
102 blue to yellow).

103 COD being mainly composed of sugars, additional organic matter was quantified through a differential COD
104 ($\text{mg O}_2.\text{L}^{-1}$) defined as:

$$105 \text{ COD}_{\text{diff}} = \text{COD} - \text{COD}_{\text{sugars}} \quad (1)$$

106 Where $\text{COD}_{\text{sugars}}$ is the COD ($\text{mg O}_2.\text{L}^{-1}$) deduced from sugar concentrations and the stoichiometry of the
107 oxidation reaction (1g.L⁻¹ of fructose and glucose corresponds to a COD of 1.066 $\text{mg O}_2.\text{L}^{-1}$ when 1 g.L⁻¹ of
108 sucrose corresponds to a COD of 1.122 $\text{mg O}_2.\text{L}^{-1}$).

109

110 UV absorbance measurement at 216.4 nm ($\text{OD}_{216.4}$) and 264.4 nm ($\text{OD}_{264.4}$) allowed evaluating the presence
111 of amino acids or peptides. Samples were diluted ten times.

112 2.3. Pre-treatment

113 Sieving at 169 μm and 79 μm followed by dead-end MF 0.6 μm was first implemented, as in Garnier *et al.*
114 (2020). The obtained turbidity remaining too high to fulfil quality requirements for further NF or RO step,
115 the permeate obtained from MF was further ultra-filtrated. Three UF organic membranes with different
116 Molecular Weight Cut-Off (MWCO), namely 100 000, 10 000 and 5 000 g.mol^{-1} , were tested therefore
117 (Table 1).

118 2.4. NF and RO membranes

119 Cauliflower processing wastewater contained sucrose ($\text{MW} = 342 \text{ g.mol}^{-1}$) and mainly glucose and fructose
120 ($\text{MW} = 180.16 \text{ g.mol}^{-1}$). Consequently, three NF membranes with MWCO between 150 and 300 g.mol^{-1} and
121 one RO membrane were selected for further purification (Table 1). New membranes were stored dry at 4 °C.

122 To remove the protective coating or storage solution, they were dipped before experiments in a 0.4 g.L^{-1}
123 KOH solution for 2 h and then in deionized water for 24 h minimum. Prior to experiments, membranes were
124 pre-compacted (20 bar, 15 min) in the filtration device.

125

126 **Table 1**

127 Overview of membranes characteristics according to manufacturer's data

Supplier	Membrane	Type	Rejection	MWCO (g.mol ⁻¹)	Active layer polymer	Maximum temperature (°C)	Maximum pressure (bar)	Pure water permeability (20°C - L.h ⁻¹ .m ⁻² .bar ⁻¹)
Alfa Laval (Elancourt, France)	FS40PP	UF	-	100 000	Fluoro polymer	60	10	78 ^a
Koch Membrane Systems Division (Lyon, France)	HFK-131	UF	-	10 000	Polyethersulfone	55	9.7	53 ^a
Koch Membrane Systems Division (Lyon, France)	HFK-328	UF	-	5 000	Polyethersulfone	55	9.7	33 ^a
GE water & process technologies (Saint-Thibault-des- Vignes, France)	DK	NF	98% 2000 ppm MgSO ₄ (7.6 bar, 25°C)	150–300	Semi-aromatic polypiperazine amide	50	41.4 bar if $\theta < 35$ °C; 30 bar otherwise	4.0 ^b
DOW France (Saint-Denis, France)	NF270	NF	97% 2000 ppm MgSO ₄ (4.8 bar, 25°C)	150–300	Semi-aromatic polypiperazine amide	45	41	14.8 ^b
Koch Membrane Systems Division (Lyon, France)	SR3D	NF	> 99.0% 5000 ppm MgSO ₄ (6.5 bar, 25°C)	200	Proprietary Thin- Film Composite polyamide	50	44.8	7.5 ^b
Hydranautics – Nitto France (Roissy, France)	ESPA4	RO	99.2% (99.0% minimum) 1500 ppm NaCl (10.3 bar, 25°C)	-	Aromatic polyamide Thin- Film Composite	45	40	6.3 ^b
(^a)	This	study;	(^b)	from	Garnier	et	al.,	2020

128

129 2.5. Membrane setup and operating conditions

130 Experiments were run using the LabStak M20 filtration device from Alfa Laval described in Garnier *et al.*
131 (2020). It allows testing several flat-sheet membranes simultaneously. The effective area for each membrane
132 was $2 \times 0.018 \text{ m}^2$.

133 To study water permeability and solutes' rejection, experiments were run in total recirculation mode:
134 deionized water filtration ($< 2 \text{ h}$) for pure water permeability measurement, wastewater filtration ($< 8 \text{ h}$), and
135 deionized water filtration *once more* (after rinsing with deionized water for 10 min minimum). For all
136 experiments, retentate flowrate was set at 300 L.h^{-1} and temperature at $20 \text{ }^\circ\text{C}$. For UF membranes, two
137 transmembrane pressures (*TMP*) were tested: 3 and 5 bar. For NF and RO membranes, *TMP* was increased
138 from 5 to 25 bar by 5 bar steps and then decreased symmetrically. Sampling and measurements were done
139 after at least 30 min run.

140 Once UF membrane selection was made, filtration was run in discontinuous mode to produce a sufficient
141 amount of ultra-filtrated permeate: the permeate stream was collected in a distinct tank and the concentrate
142 returned to the feed tank until reaching the desired volume reduction ratio (*VRR*):

$$143 \quad VRR = \frac{V_i}{V_f} \quad (2)$$

144 Where V_i is the initial volume in the feed tank and V_f the final volume.

145 3. Filtration efficiency and solution-diffusion model application

146 Filtration efficiency was estimated by the permeate flux J_p (m.s^{-1} or $\text{L.h}^{-1}.\text{m}^{-2}$) evolution with *TMP*, as well as
147 by the solutes' rejections Tr_i , calculated for each solute or parameter i (COD, COD_{diff} , total nitrogen, OD,
148 sugars, ions).

$$149 \quad J_p = \frac{Q_p}{S} \quad (3)$$

$$150 \quad Tr_i = \frac{C_{r,i} - C_{p,i}}{C_{r,i}} \quad (4)$$

151 Where Q_p ($\text{m}^3.\text{s}^{-1}$ or L.h^{-1}) is the permeate flow rate, S (m^2) is the effective membrane area and $C_{r,i}$ and $C_{p,i}$
152 (mol.m^{-3}) are the concentrations of solute i respectively in the retentate and in the permeate.

153

154 Experimental solute i flux (J_i ($\text{mol. s}^{-1}.\text{m}^{-2}$)) through the membrane was calculated according to:

$$155 \quad J_i = C_{p,i} \times J_p \quad (5)$$

156 The Solution-Diffusion (*SD*) model is commonly used for describing the transport of non-ionic organic
157 solutes through dense membranes such as RO and tight NF ones (Nguyen, D. *et al.*, 2016; Qasim *et al.*, 2019;

158 Wijmans and Baker, 1995). For diluted solutions and in the absence of irreversible fouling, this model can be
 159 simplified to predict J_p and J_i , provided the water and solutes permeabilities are known. When **concentration**
 160 **polarization** is considered on the retentate side (Aimar et al., 2010), the following **equation arises for the**
 161 **permeate flux**:

$$162 \quad J_p = A_w \times [TMP - \Delta\pi] \quad (6)$$

163 Where A_w ($\text{m.s}^{-1}.\text{Pa}^{-1}$ or $\text{L.h}^{-1}.\text{m}^2.\text{bar}^{-1}$) is the pure water permeability, $TMP = \frac{P_f + P_r}{2} - P_p$ (Pa or bar) is the
 164 transmembrane pressure (P_f , P_r and P_p are the pressures in the feed, the retentate and the permeate,
 165 respectively (bar)), and $\Delta\pi = \pi_{r,m} - \pi_p$ (Pa or bar) is the osmotic pressure gradient between the membrane
 166 interface in the retentate (considering concentration polarization) and the permeate.

167 A_w could be deduced with Eq. 6 for pure water filtration experiments at different TMP , before and after
 168 effluent treatment on the membrane.

169 With the same SD model, solute i flux is given by:

$$170 \quad J_i = B_i \times [C_{r,m,i} - C_{p,i}] \quad (7)$$

171 Where B_i (m.s^{-1}) is the membrane permeability to solute i and $C_{r,m,i}$ (mol.m^{-3}) is its concentration at the
 172 membrane interface in the retentate, that can be estimated through the film model theory:

$$173 \quad C_{r,m,i} = C_{p,i} + [C_{r,i} - C_{p,i}] \times \exp\left(\frac{J_p}{k_i}\right) \quad (8)$$

174 Where k_i (m.s^{-1}) is the mass transfer coefficient of solute i in the polarization layer.

175

176 To assess the simplified Solution-Diffusion model and determine k_i , and B_i , eq. (5), (7) and (8) were
 177 combined to give:

$$178 \quad \ln\left(\frac{C_{p,i} \times J_p}{C_{r,i} - C_{p,i}}\right) = \ln(B_i) + \frac{J_p}{k_i} \quad (9)$$

179 Plotting $\ln\left(\frac{C_{p,i} \times J_p}{C_{r,i} - C_{p,i}}\right)$ vs J_p led to the graphical determination of B_i and k_i .

180 4. Results and Discussion

181 4.1. Characterisation of raw wastewater

182 Cauliflower processing wastewater had a particular odour which could be attributed to sulphur and N-
 183 bearing molecules, and foaming attested the presence of proteins. Table 2 shows the composition of the
 184 blanching wastewater (two samples). The difference between total and dissolved COD was within the
 185 accuracy limit.

186 Fructose and glucose represented respectively 72% and 46% of the total COD of the raw wastewater,
187 showing its variability. These proportions increased to 99% and 79% when raw wastewater was micro
188 filtrated, indicating that these are the main dissolved organic substances present. Other organic dissolved
189 substances were estimated by UV spectrophotometry at 216.4 nm (possibly corresponding to peptide bonds)
190 and 264.4 nm (corresponding to aromatic rings), as well as by TN measurement. These may be amino acids
191 or peptides/proteins containing aromatic rings like histidine, phenylalanine, tryptophan and tyrosine, present
192 in cauliflowers.

193 By comparing the composition of wastewater with that of typical cauliflower (Table 2), the transfer of sugars
194 and most minerals (phosphate, sulphate, sodium, potassium, magnesium and calcium) into wastewater during
195 blanching is confirmed. Glucose and fructose are transferred in the same proportion. Sucrose, present in
196 small amounts in cauliflower (Bhandari and Kwak, 2015) is also transferred into the wastewater.

197 As in the study on carrot wastewater (Garnier et al., 2019; Garnier et al., 2020), TSS, COD, conductivity,
198 fructose, glucose and sucrose were selected as key parameters. Concerning the French drinking water
199 standard and regarding ions, only ammonium was out of the range (8–12 mg.L⁻¹ in raw wastewater vs 0.1
200 mg.L⁻¹ in French standard), so it was selected as another key parameter. The other ions were merged as key
201 parameter “conductivity”. As raw wastewater was white with an orange tint, color was also monitored.

202

203

204

205 **Table 2**

206 Characteristics and composition of cauliflower blanching raw wastewater (two samples from cauliflower
 207 blanching), cauliflower and drinking water

Parameter	Raw wastewater	Cauliflower (USDA*)	Drinking water (French standard)	Drinking water (factory)
Temperature (°C)	50 – 80	ni	≤ 25	nd
TSS (mg.L ⁻¹)	150 – 290	ni	-	nd
Total COD (mg O ₂ .L ⁻¹)	7 410 – 10 120	ni	-	3.8
Dissolved COD (mg O ₂ .L ⁻¹)	7 560 – 10 290	ni	-	nd
Total Nitrogen (mg N.L ⁻¹)	190 – 265	ni	-	nd
Conductivity (μS.cm ⁻¹)	2 420 – 2 640	ni	180 – 1 000	261
pH	5.8 – 5.9	ni	6.5 – 9	6.86
Turbidity (NTU)	45 – 125	ni	≤ 0.5	< 0.1
Color	L* =66 – 90 a* = 11 – 23 b* = 11 – 21	ni	Acceptable to consumers and no abnormal change	nd
UV absorbance	OD _{216.4} = 2 200 – 2 360 OD _{264.4} = 950 – 1 230	ni	-	nd
Carbonate hardness (°f)	24.5 – 23.5	ni	-	3.5
Fructose	2 130 – 2 210 mg.L ⁻¹	0.97 g/100g	-	absence
Glucose	1 930 – 2 190 mg.L ⁻¹	0.94 g/100g	-	absence
Sucrose	170 – 630 mg.L ⁻¹	0 g/100g	-	absence
Cl ⁻ (mg.L ⁻¹)	110 – 140	ni	≤ 250	42
NO ₂ ⁻ (mg.L ⁻¹)	< LOD	ni	≤ 0.5	< LOD
NO ₃ ⁻ (mg.L ⁻¹)	16 – 21	ni	≤ 50	5
SO ₄ ²⁻ (mg.L ⁻¹)	100 – 140	ni	≤ 250	15
PO ₄ ³⁻	80 – 100 mg.L ⁻¹	P: 44 g/100g	-	< LOD
Na ⁺	32 – 40 mg.L ⁻¹	30 g/100g	≤ 200	19
NH ₄ ⁺ (mg.L ⁻¹)	8 – 12	ni	≤ 0.1	< LOD
K ⁺	1 030 – 1 050 mg.L ⁻¹	299 g/100g	-	4
Mg ²⁺	34 – 44 mg.L ⁻¹	15 g/100g	-	6
Ca ²⁺	78 – 92 mg.L ⁻¹	22 g/100g	-	22

208 * <https://fdc.nal.usda.gov/fdc-app.html#/food-details/170393/nutrients> published 4/1/2019.

** ni: not indicated, nd: not determined

209 4.2. Pre-treatment selection

210 The removal efficiency of the sieving-MF pre-treatment was 60% for TSS, 34% for COD, 17% for OD_{216.4},
211 39% for OD_{264.4} and null for sugars. Nevertheless, the residual turbidity (average 48 NTU) was too high for
212 feeding a NF or RO process. Additional pre-treatment with UF membrane (MWCO of 100 000, 10 000 or
213 5 000 g.mol⁻¹) was then experienced on microfiltration permeate. Whatever the pressure (3 and 5 bar) and the
214 membrane, the residual turbidity was below 0.5 NTU, complying with the recommendations of the NF and
215 RO manufacturers. Membrane FS40PP with the highest MWCO (100 000 g.mol⁻¹) and a 3 bar pressure was
216 preferred as it limited permeability loss during the filtration stage (41%, against 68% and 62% with
217 membranes of 10 000 and 5 000 g.mol⁻¹ MWCO, respectively).

218 Finally, the removal efficiency of this pre-treatment (sieving + microfiltration + ultrafiltration on FS40PP at
219 VRR 3.5) reached 99% for turbidity, 50% for COD, 12% for COD_{diff}, 42% for TN, 40% for conductivity,
220 26% for OD_{216.4} and 49% for OD_{264.4}. The decrease in sugar concentrations was unexpected: 56% for
221 fructose, 98% for glucose and 100% for sucrose. This result was due to fermentation (Paramithiotis et al.,
222 2010) during storage even if mostly at 4°C, detected by the decrease of pH and chlorine concentration, and
223 confirmed by specific acetate and lactate peaks on HPIC chromatograms.

224 4.3. NF and RO performances

225 4.3.1. Critical flux, concentration polarization and fouling

226 All the following experiments were performed with pure water or with the pre-treated wastewater produced
227 as described in section 4.2. Results are presented on Fig. 2, from which pure water permeability A_w could be
228 deduced according to Eq. 6 (with $\Delta\pi = 0$) (Table 3). For SR3D and ESPA4 membranes, A_w values before
229 effluent filtration were similar to those in Garnier et al (2020) (Table 1), while they appeared much lower or
230 higher respectively for NF270 (-30%) and DK (+ 45%).

231 A small A_w decrease was observed after NF or RO treatment proving that fouling had occurred during
232 effluent treatment. For wastewater filtration at the lowest TMP values, the relation between J_P and TMP was
233 linear, showing that no fouling had yet occurred but only a reversible concentration polarization phenomenon
234 (eq. 8) (Aimar, 2006). Above a given flux value, named the critical flux, it was no longer linear meaning that
235 irreversible concentration polarization occurred together with a likely irreversible fouling (Aimar et al.,
236 2010). The critical flux and corresponding pressure obtained graphically (Table 4) show that membranes do
237 not differ from each other on these parameters but rather on A_w level (Table 3). To confirm the fouling
238 phenomenon, J_P was studied over time and compared with initial pure water flux: for each TMP applied up
239 to 15 bar, flux measurements were made after 5 min (initial flux) and 30 min; for 25 bar, it was after 5, 15
240 and 30 min. TMP was then decreased (20, 15, 10, 5 and 1 bar) and a measurement was made after 10-min
241 run. As shown in Fig. 2, during pressure increase and below the critical flux, the steady state was quickly
242 reached as the permeate flux was almost the same after 5 and 30 min. On the contrary, for NF270 membrane

243 and above the critical flux, a decrease of up to 10% of J_p was observed over time (Fig. 2a). Moreover,
 244 hysteresis appeared for all membranes when TMP was decreased, confirming that critical flux had been
 245 exceeded and that fouling had developed (Aimar et al., 2010).

246

247 **Table 3**

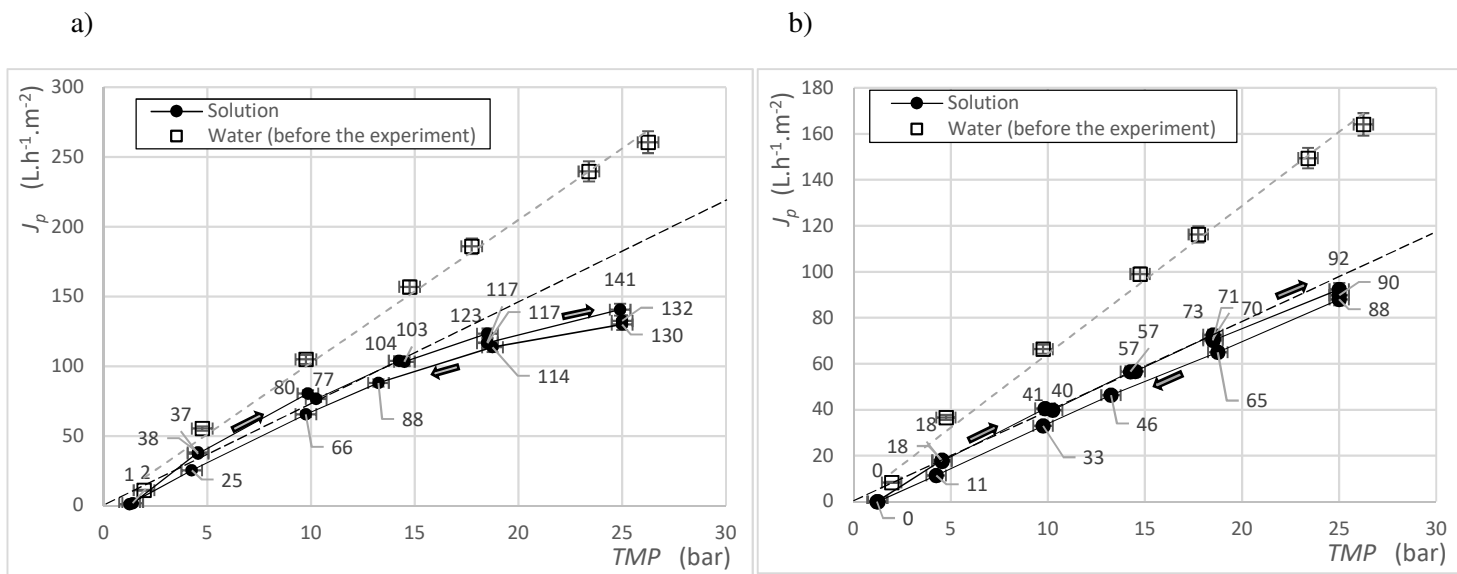
248 Pure water permeability A_w before and after NF and RO treatment

Supplier	Membrane	Type	A_w measured at 20°C (L.h ⁻¹ .m ⁻² .bar ⁻¹)	
			Before effluent filtration	After effluent filtration
DOW	NF270	NF	10.4 ± 0.4	8.9 ± 0.3
Koch	SR3D	NF	7.0 ± 0.2	6.4 ± 0.2
GE	DK	NF	5.8 ± 0.2	5.3 ± 0.2
Hydranautics	ESPA4	RO	6.4 ± 0.2	5.3 ± 0.2

249

250

251



252

253 **Fig. 2.** Permeate flux for pure water and cauliflower pre-treated wastewater, highlighting hysteresis - J_p
 254 values obtained over time are indicated directly on the points:

255

(a) NF270 membrane (b) ESPA4 membrane.

256

257

258

259 **Table 4**

260 Critical flux and corresponding pressure for NF and RO membranes

Membrane	NF270	SR3D	DK	ESPA4
Critical flux (L.h ⁻¹ .m ⁻²)	100	100	90	90
Pressure at critical flux (bar)	15	18	19	24

261 *4.3.2. Solutes rejections*

262 The rejection performances of the membranes were compared before and after the critical flux as both
 263 concentration polarization and fouling might have a beneficial or detrimental impact on membrane
 264 selectivity (Aimar et al., 2010). Rejections of COD, glucose and fructose versus permeate flux are given Fig.
 265 3. After pre-treatment, sucrose concentrations were below the quantification limit and were not considered.
 266 As expected, RO gave the highest rejections. For NF, rejections decreased with MWCO increase (Table 1),
 267 assessing that size exclusion was the major mechanism for NF membranes. DK and NF270 showed
 268 comparable patterns.

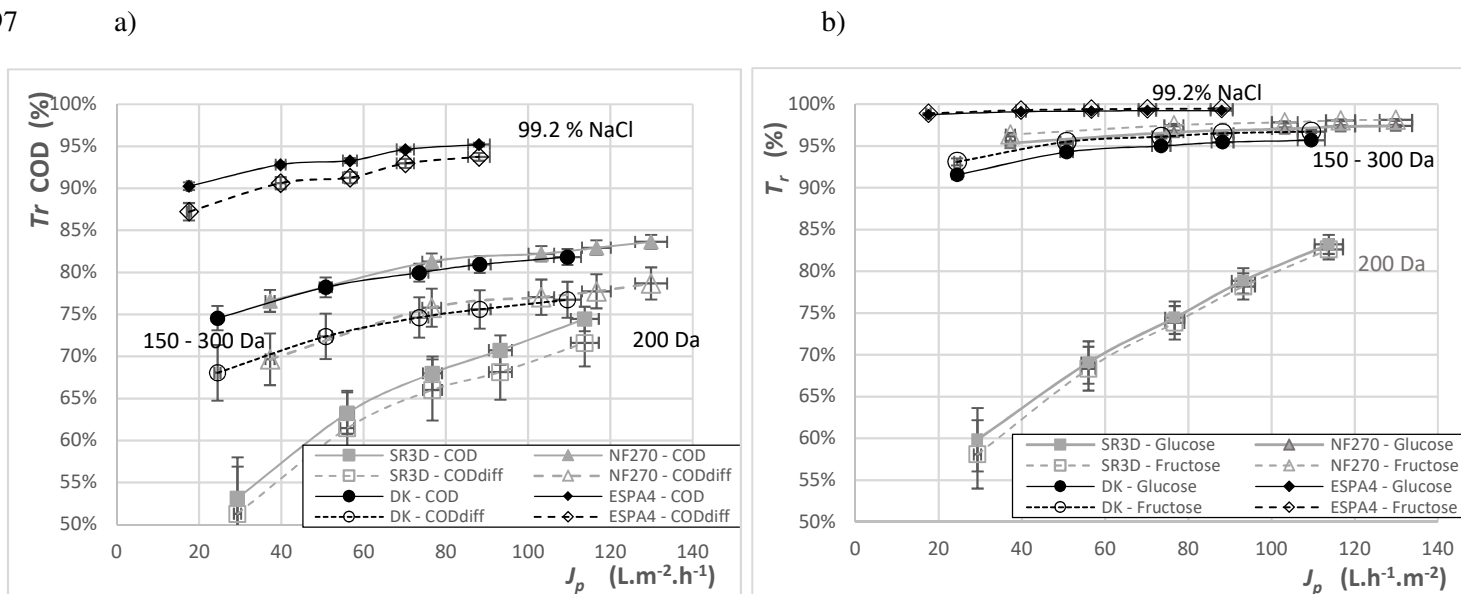
269 The COD rejections for DK (150–300 g.mol⁻¹), NF270 (150–300 g.mol⁻¹), SR3D (200 g.mol⁻¹) and ESPA4
 270 (99.2% NaCl) membranes increased with *TMP* from 74.6% to 81.8%, 76.6% to 83.6%, 53.2% to 74.5% and
 271 90.3% to 95.2%, respectively (Fig. 3-a). At 25 bar, the minimal COD values in the permeate remained high
 272 for NF (above 700 mg O₂.L⁻¹), and much lower for ESPA4 (208 mg O₂.L⁻¹). COD rejections continually
 273 increased but more and more slowly showing that exceeding the critical flux (between 90 and 100 L. h⁻¹.m⁻²)
 274 is not efficient. For fructose and glucose (87–89% and 11–13% of total sugars in the retentate, respectively)
 275 the same membrane ranking was observed (Fig. 3-b). The rejections were at least 95% for NF270, 91% for
 276 DK and 98% for ESPA4 membrane which was consistent with other studies on sugars (Garnier et al., 2020;
 277 Nguyen et al., 2015). Low rejection (58 to 86%) was observed for SR3D confirming a different behaviour, as
 278 already noticed on carrot processing wastewater for protons, amino-acid-type and bicarbonates (Garnier et
 279 al., 2020). COD_{diff} rejection was always lower than the COD rejection (Fig. 3-a) which suggested that
 280 organic non-sugar molecules showed poor rejection. To investigate this, the rejections of TN, OD_{216.4} and
 281 OD_{264.4} were examined and compared with that for COD and COD_{diff} (Fig. 4). Results for NF270 membrane
 282 were not presented, as it behaves like DK membrane.

283 OD_{216.4} rejections were below COD rejections for SR3D (200 g.mol⁻¹), similar for NF270 and DK (150–300
 284 g.mol⁻¹) and above for ESPA4 membrane. This suggests that size exclusion was the main selectivity factor
 285 and that OD_{216.4} represents non-aromatic and non-sugar molecules with molecular weight below 150 g.mol⁻¹
 286 (Fig. 4). For ESPA4 membrane (RO), OD_{216.4}, OD_{264.4} and TN rejections were above COD_{diff} rejection
 287 suggesting that small and undetermined molecules migrate through the membrane (Fig. 4-c). For all
 288 membranes, OD_{264.4} rejections were similar and slightly above TN rejections suggesting that the main part of
 289 nitrogen compounds detected by TN measurements absorb at 264.4 nm and would thus contain aromatic
 290 amino acids identified in cauliflower (Table 5). OD_{264.4} rejections of SR3D, NF270 and DK membranes were

291 respectively between 65.0% and 80.9%, 89% and 91.7% and 87.8% and 90.1%, consistent with MW of those
 292 aromatic amino acids and MWCO of the membranes. They appeared to be better rejected by ESPA4
 293 membrane, with OD_{264.4} rejections between 96.8% and 100%. OD_{216.4} rejections were always below OD_{264.4}
 294 and TN rejections, showing that non-aromatic amino acids partially transfer through NF membranes,
 295 probably due to smaller MW.

296

297



298

Fig. 3. COD and sugars rejection versus permeate flux (20°C, feed flow rate = 300 L.h⁻¹):

299

(a) COD and COD_{diff} (b) glucose and fructose.

300

Table 5

301

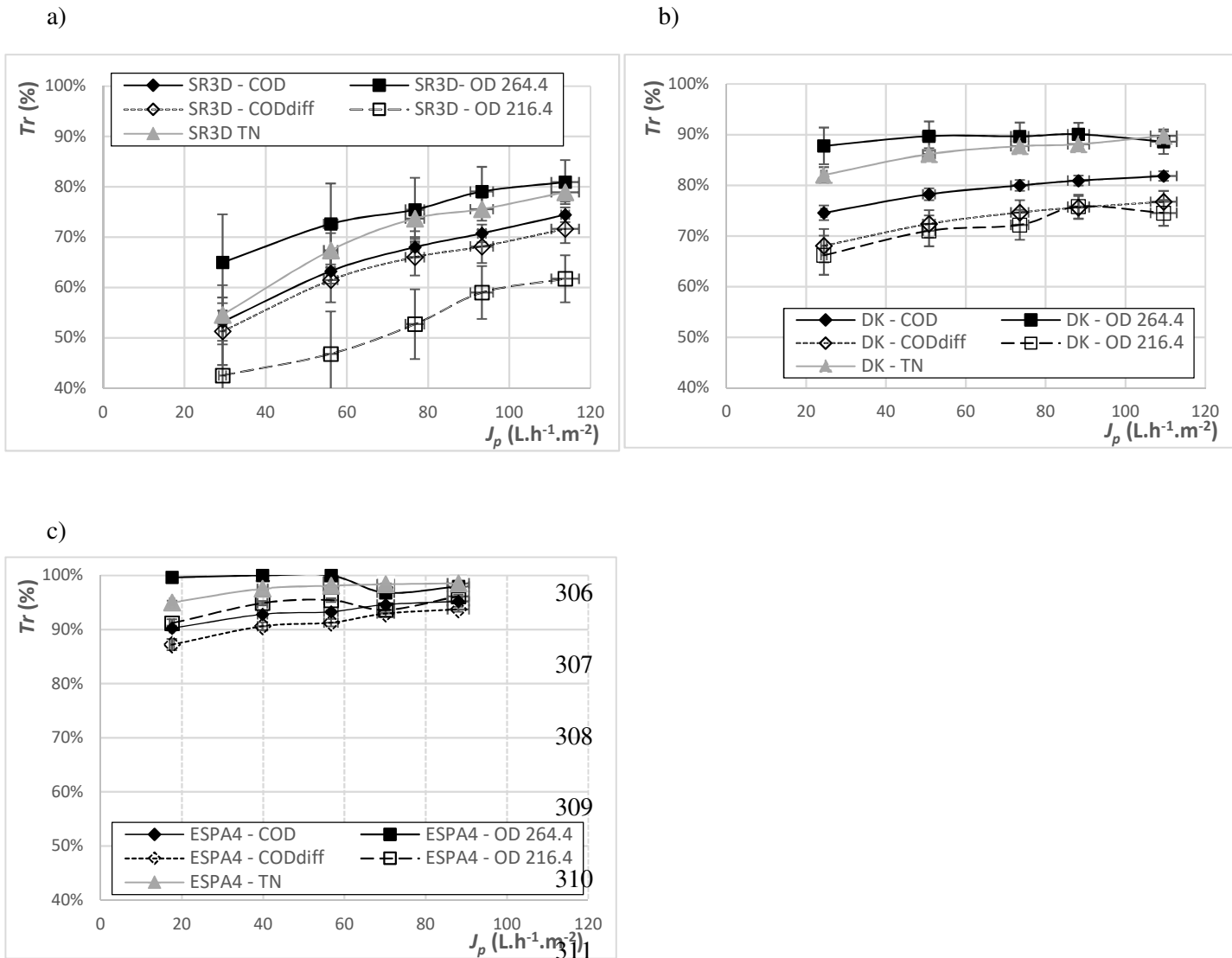
Main amino acids and aromatic amino acids in cauliflowers and their properties

Main Amino acids	Concentration in cauliflower (USDA) (g / 100 g)	Solubility in water at 25°C (g / 100 g)	Molecular weight (g.mol ⁻¹)	Isoelectric point	Net charge at pH = 4.7
Glutamic acid	0.245	0.9	147.1	3.22	Negative
Aspartic acid	0.216	0.5	133.1	2.77	Negative
Leucine	0.107	2.4	131.2	5.98	Positive
Lysine	0.099	0.6	146.2	9.74	Positive
Alanine	0.097	16.7	89.1	6.01	Positive
Serine	0.096	25	105.1	5.68	Positive
Valine	0.092	8.8	117.1	5.96	Positive
Proline	0.079	162.5	115.1	6.30	Positive
Aromatic amino acids (16% w/w of total amino acids in cauliflower)					
Phenylalanine	0.066	2.79	165.2	5.48	positive

Tyrosine	0.04	0.05	181.2	5.66	positive
Histidine	0.037	4.35	155.1	7.59	Positive

302

303



304

305

312

Fig. 4. COD, COD_{diff}, TN, OD_{216.4} and OD_{264.4} rejection versus permeate flux

313

(20°C, feed flow rate = 300 L.h⁻¹): (a) SR3D membrane (b) DK membrane (c) ESPA4 membrane.

314

315

4.3.3. Minerals rejection

316

Rejections of sulphate and magnesium for NF270 and DK membranes were consistent with manufacturer data (Table 6). Differences can be due to operating concentrations and pressures, or to model solutions (and not complex effluents) used by manufacturers. Again, different behaviour of SR3D was observed with sulphate rejection (69.7% instead of 99%). For all minerals (Table 7), this membrane generally gave lower rejections than other NF membranes (NF270 and DK).

321

322

323

324 **Table 6**

325 Magnesium (Mg^{2+}) and sulphate (SO_4^{2-}) rejections with NF membranes à 4.6 bar

		NF270	DK	SR3D
This study	Mg^{2+} rejections	96.0 %	96.0 %	64.0 %
	SO_4^{2-} rejections	99.2 %	99.1 %	69.7 %
Manufacturer's data		97% at 4.8 bar 2 000 ppm $MgSO_4$	98% at 7.6 bar 2 000 ppm $MgSO_4$	> 99% at 6.5 bar 5 000 ppm $MgSO_4$

326

327 Ionic mass balances were established for the retentate and the permeate for DK and ESPA4 (Table 7), both at
328 19 bar. As in Garnier et al. (2020), for both membranes the sum of the negative charges was far lower than
329 the positive ones, especially in the retentate and with DK. This difference can be explained by the presence
330 of negatively charged molecules at the pH of the pre-treated effluent (pH 4.7), such as amino acids (Table 5)
331 or organic acids (lactic acid, pKa 3.86) that were detected but not quantified in the effluent. Consequently,
332 cations appeared globally more retained than anions in the case of the DK membrane, which can be an
333 artifact of this proportion of negative ions not quantified in the retentate.

334 For DK membrane, the main identified compounds that transferred through the membranes were HCO_3^- , Cl^-
335 and K^+ . For ESPA4, the only RO membrane, it was Cl^- and K^+ (but below 5%). ESPA4 exhibited the best
336 rejections ($\geq 95\%$) due to its more selective polyamide layer, much thicker than that of NF membranes
337 (Freger, 2003).

338

339

340

341

342

343

344

345

346

347

348

349

350 **Table 7**351 **Ionic mass balance and rejection for DK and ESPA4 membranes at 19 bar**352 (Note: with the Labstak pilot C_r is the same for both membranes)

Minerals	C_r (mmol.L ⁻¹)	DK		ESPA4	
		C_p (mmol.L ⁻¹)	Tr (%)	C_p (mmol.L ⁻¹)	Tr (%)
HCO ₃ ⁻	2.27	1.35	40.3	0.00	100.0
Cl ⁻	1.97	0.94	52.0	0.07	96.7
NO ₃ ⁻	0.15	0.09	41.7	0.02	89.3
H ₂ PO ₄ ⁻	0.49	0.02	96.9	0.00	100.0
SO ₄ ²⁻	0.71	0.00	100	0.00	99.8
Sum of negative charges	6.29 meq.L⁻¹	2.43 meq.L⁻¹	61.4	0.08 meq.L⁻¹	98.7
Na ⁺	0.90	0.31	65.7	0.01	99.0
NH ₄ ⁺	0.37	0.21	44.7	0.02	94.4
K ⁺	11.11	4.56	58.9	0.25	97.8
Mg ²⁺	0.82	0.01	98.5	0.00	99.8
Ca ²⁺	1.10	0.03	97.6	0.00	99.7
H ⁺	Negligible	Negligible	-	Negligible	-
Sum of positive charges	16.21 meq.L⁻¹	5.15 meq.L⁻¹	68.2	0.29 meq.L⁻¹	98.2
<u>Negative charges missing</u>	9.91 meq.L ⁻¹	2.72 meq.L ⁻¹		0.21 meq.L ⁻¹	

353

354

355 Rejections of the main **monovalent** (Fig. 5) and **divalent ions** (Fig. 6) are presented separately. Due to their
356 low concentration in the raw wastewater (Table 2), ammonium, sodium and nitrate rejections are not
357 presented. At the pH of the effluent (4.7) and based on its equilibrium diagram, **phosphate was mainly in**
358 **H₂PO₄⁻ form.**

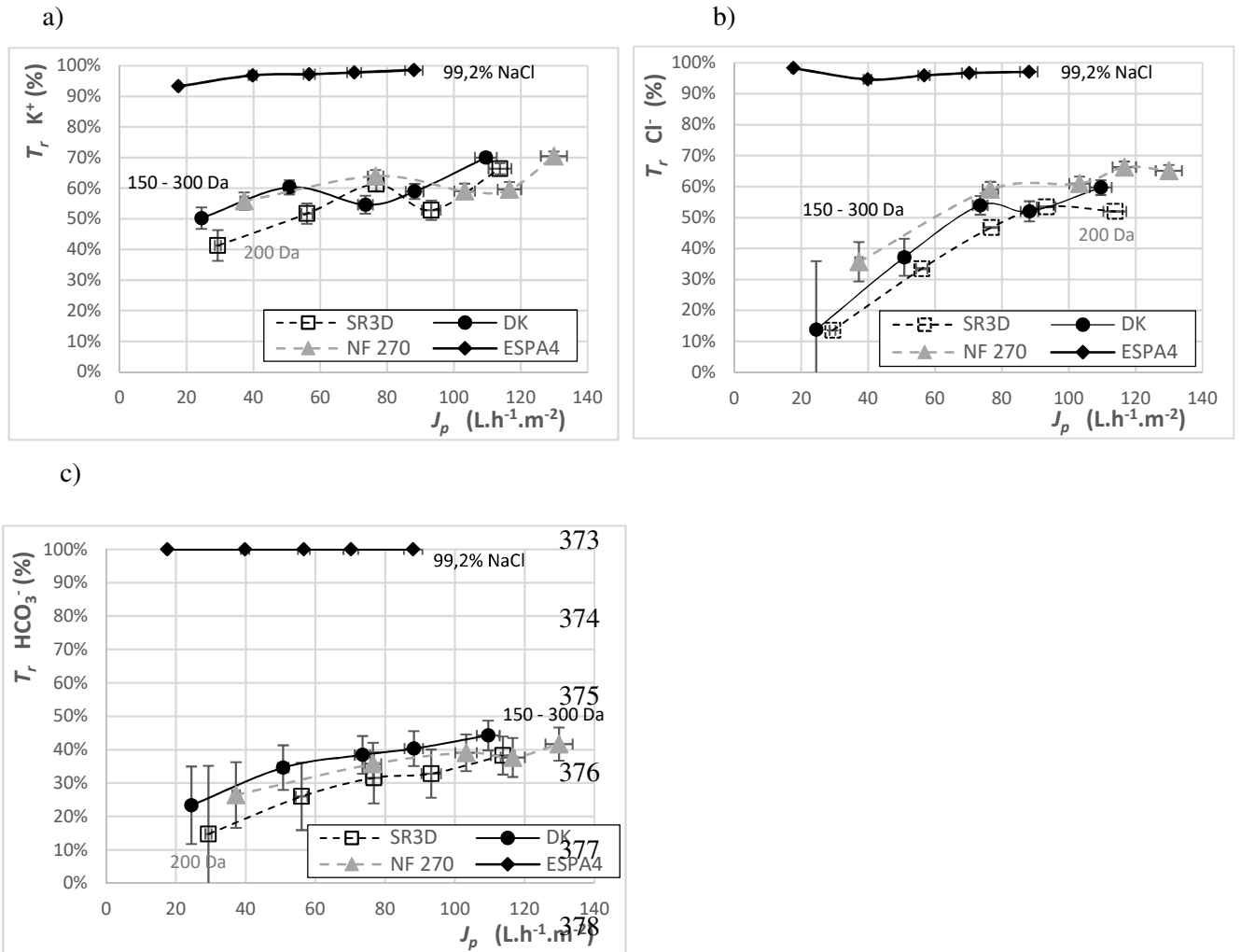
359 **Whichever membrane was used**, rejections of monovalent ions (Na⁺, K⁺, Cl⁻, NO₃⁻, HCO₃⁻) were generally
360 between 20 and 60%, much lower than that of divalent ions (Ca²⁺, Mg²⁺, SO₄²⁻), above 70%. This is
361 consistent with the Donnan space charge model (Aimar, 2006), **based on electrostatic repulsions and**
362 **considering the ions' valence.** Moreover, for two ions with the same charge but different radii, the one
363 having the highest charge density would exhibit the highest rejection (Epsztein et al., 2018). This may
364 explain the highest rejection of Cl⁻ as compared to NO₃⁻, or that of Na⁺ as compared to NH₄⁺, due to their
365 respective ionic radii (Lide, 2004; Shannon, 1976). Far more H₂PO₄⁻ is rejected due to its higher molecular
366 weight (MW = 98 g.mol⁻¹).

367 ESPA4 led to the best rejections, at about 100% for divalent ions and above 95% for monovalent ones
 368 provided pressure was above 10 bar (or J_p above 40 L.h⁻¹.m⁻²).

369

370

371



372

379 **Fig. 5.** Monovalent ions rejection versus permeate flux (20°C, feed flow rate = 300 L.h⁻¹):

380

(a) K⁺ (b) Cl⁻ (c) HCO₃⁻.

381

382

383

384

385

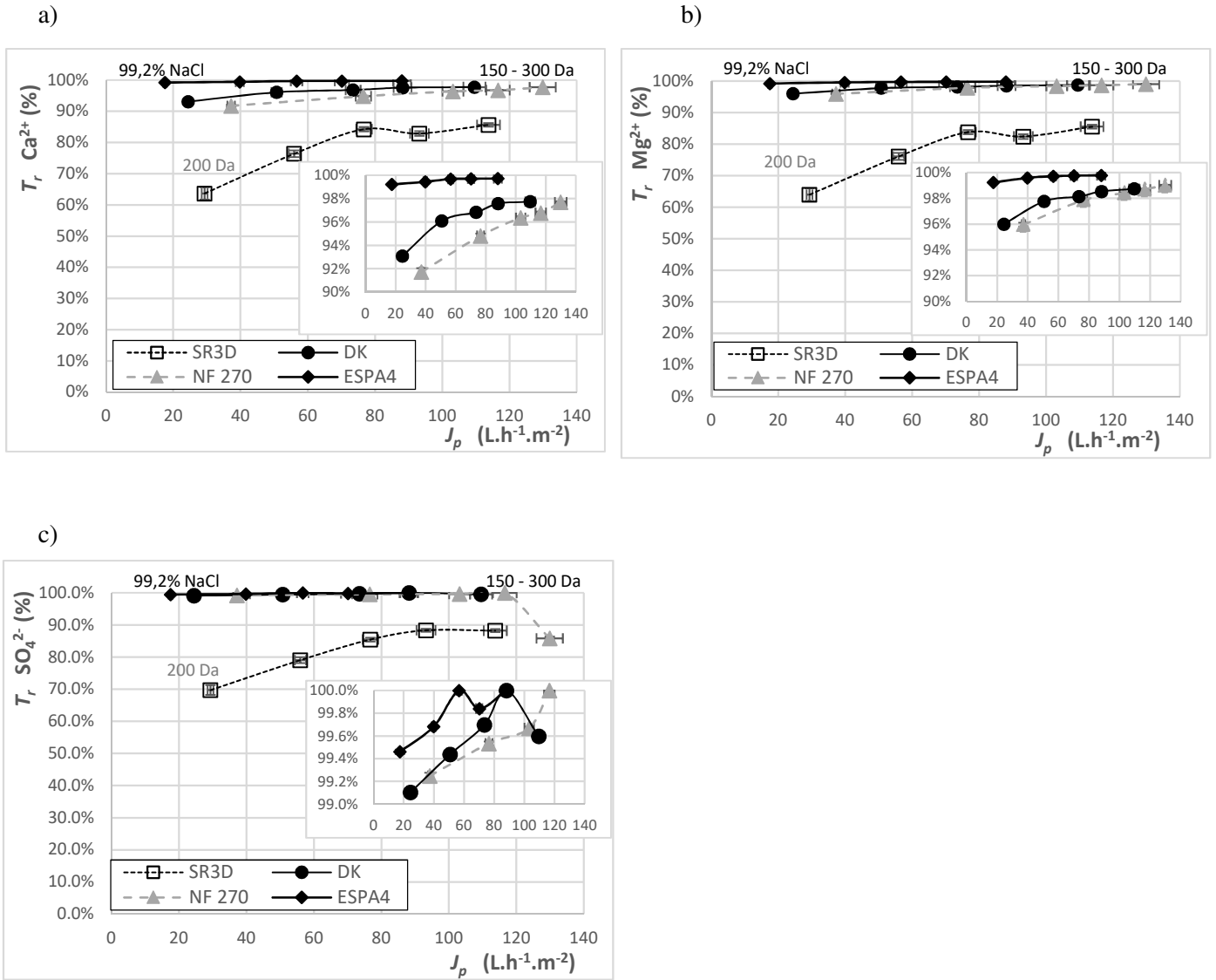
386

387

388

389

390



391

392

400

Fig. 6. Divalent ions rejection versus permeate flux (20°C, feed flow rate = 300 L.h⁻¹):

401

(a) Ca^{2+} (b) Mg^{2+} (c) SO_4^{2-} .

402

4.3.4 Choice of NF or RO membranes for the reconditioning treatment

403

404

405

406

407

408

409

410

Comparable results were observed with NF270 and DK membranes and lower performance (lower rejections) with SR3D membrane. NF270 at $TMP = 15$ bar and DK at $TMP = 19$ bar (pressure at critical flux) appeared as the best compromises for COD rejection and permeate flux. With RO membrane (ESPA4), the rejections were higher and critical flux corresponded to $TMP = 24$ bar (Table 4). To obtain the best compromise between COD rejection and permeate flux and to ensure a residual COD in the permeate below 400 mg O₂.L⁻¹, ESPA4 membrane was selected at about 19 bar. The permeate quality indicators are summarized in Table 8. For an equivalent permeate flux, the ESPA4 treatment of complex carrot peeling effluent at about 15 bar had allowed a better permeate quality (Garnier et al., 2020). This can be explained by

411 the much lower organic load of the carrots processing wastewater (Table 9), similar rejections leading to
 412 lower concentrations in the permeate. An additional explanation may be a higher fermentation of sugar due
 413 to longer storage in the case of cauliflower processing wastewater, leading to an increase in small
 414 metabolites content such as acetic or lactic acids, which can permeate through the membrane.

415 **Table 8**

416 Permeate quality for selected membranes and optimized conditions

	NF270 (NF)	DK (NF)	ESPA4 (RO)
Optimum <i>TMP</i> (bar)	15	19	19
J_p (L.h ⁻¹ .m ⁻²)	103	88	70
Total COD (mg O ₂ .L ⁻¹)	733	797	225
TN (mgN.L ⁻¹)	15	17	2
Conductivity (μS.cm ⁻¹)	512	527	83
pH	5.1	4.9	3.8
Carbonate Hardness (°f)	14.2	13.5	< 2
Fructose (mg.L ⁻¹)	18	31	5
Glucose (mg.L ⁻¹)	3	5	1
Sucrose (mg.L ⁻¹)	< 1	< 1	< 1
Cl ⁻ (mg.L ⁻¹)	26	33	2
NO ₃ ⁻ (mg.L ⁻¹)	7	6	1
PO ₄ ³⁻ (mg.L ⁻¹)	< 1	1	< 1
SO ₄ ²⁻ (mg.L ⁻¹)	< 1	< 1	< 1
Na ⁺ (mg.L ⁻¹)	7	7	< 1
NH ₄ ⁺ (mg.L ⁻¹)	3	4	< 1
K ⁺ (mg.L ⁻¹)	177	178	10
Mg ²⁺ (mg.L ⁻¹)	< 1	< 1	< 1
Ca ²⁺ (mg.L ⁻¹)	2	1	< 1
OD _{216.4}	0.445	0.404	0.106
OD _{264.4}	0.031	0.040	0.012
Color	L* = 100.1 a* = 0.0 b* = 0.1 (colorless)	L* = 100.0 a* = 0.0 b* = 0.1 (colorless)	L* = 100.1 a* = 0.0 b* = 0.0 (colorless)

417

418

419

420

421

422 **Table 9**

423 Rejection efficiency of RO treatment with ESPA4

	Carrot / $TMP = 15$ bar (from Garnier et al., 2020)			Cauliflower / $TMP = 19$ bar		
	Retentate	Permeate	Tr_i (%)	Retentate	Permeate	Tr_i (%)
COD (mg O ₂ .L ⁻¹)	620	12	98.0	4 179	225	94.6
Sucrose (mg.L ⁻¹)	305	2	99.4	2	< 0.5	> 99.5
Glucose (mg.L ⁻¹)	61	0.5	99.2	114	1	99.2
Fructose (mg.L ⁻¹)	67	0.6	99.2	889	5	99.4

424 *4.4. Sugars' transfer modelling*

425 For glucose and fructose with the SR3D membrane, $\ln\left(\frac{C_{p,i} \times J_p}{C_{r,i} - C_{p,i}}\right)$ vs J_p plot was not linear (eq. 9),
426 demonstrating that the Solution-Diffusion model was not applicable and confirming the singularity of this
427 membrane. On the contrary, for the DK, NF270 and ESPA4 membranes, high R^2 values (0.91 to 0.99) were
428 obtained. k_i and B_i at 293.15 K and 300 L.h⁻¹ feed flowrate obtained for sugars are summarized in Table 10
429 and compared with those extracted from results obtained in similar operating conditions with carrot
430 processing wastewater (Garnier et al., 2020). For both effluents, $B_{i \text{ glucose}}$ was similar to $B_{i \text{ fructose}}$, at about 0.45
431 $\times 10^{-6}$ m.s⁻¹ for DK and 0.3 $\times 10^{-6}$ m.s⁻¹ for NF270. As observed in Almazan (2015), concentration of sugars
432 did not affect B_i . As expected, for dense RO membrane (ESPA4), $B_{i \text{ Glu/Fru}}$ was much lower than for NF
433 membranes, at $B_{i \text{ Glu/Fru}} = 0.1 \times 10^{-6}$ m.s⁻¹ for cauliflower wastewater, twice that for carrot ($B_{i \text{ Glu/Fru}} = 0.05 \times$
434 10^{-6} m.s⁻¹). However, it may be underlined that for this membrane, rejection was quite constant with J_p , lying
435 between 99.0 and 99.5 %, which made inaccurate k_i and B_i determination. Other studies on glucose rejection
436 with DK membrane allowed $B_{i \text{ glucose}}$ parameter to be extracted (Table 11). They lie between 0.25 and 0.95 \times
437 10^{-6} m.s⁻¹, with an average at 0.55 $\times 10^{-6}$ m.s⁻¹, consistent with the average value of 0.45 $\times 10^{-6}$ m.s⁻¹ in this
438 work, despite the diverse compositions of the studied solutions.

439 For NF membranes, k_i values increased with retentate concentrations. It was quite the opposite for RO
440 membrane: respectively for fructose and glucose, 23 $\times 10^{-6}$ and 18 $\times 10^{-6}$ m.s⁻¹ in cauliflower effluent with
441 higher concentrations compared to 42 $\times 10^{-6}$ and 40 $\times 10^{-6}$ m.s⁻¹ in carrot processing effluent (with lower
442 concentrations).

443 For all the membranes investigated and cauliflower or carrot wastewaters, B_i was far lower than k_i ($40 < k_i/B_i$
444 < 460) and especially for ESPA4 (k_i/B_i between 360 and 460), showing that the resistance to transfer was
445 logically mainly due to diffusion inside the membrane, increasingly with RO membranes due to their higher
446 density. Moreover, $C_{r \text{ mi}} / C_r$ ratios for glucose and fructose increased with TMP respectively from 1.2 to 2.9
447 (2.3 at 19 bar) and from 1.3 to 4.0 (3.0 at 19 bar) confirming the polarisation concentration.

448

449 **Table 10**

450 k_i and B_i for fructose and glucose from the simplified Solution-Diffusion model (eq. 9) for cauliflower ([this](#)
 451 [study](#)) and carrot wastewater (from results in Garnier [et al.](#), 2020).

Solute		Fructose		Glucose	
Vegetable of raw wastewater		Cauliflower	Carrot	Cauliflower	Carrot
Concentration range (mg.L ⁻¹)		830 – 926	63 – 69	112 – 124	59 – 63
pH		4.8	7.5	4.8	7.5
DK	k_i (m.s ⁻¹ x 10 ⁻⁶)	33	19	30	18
	B_i (m.s ⁻¹ x 10 ⁻⁶)	0.42	0.45	0.52	0.42
	k_i/B_i	78	42	58	43
NF270	k_i (m.s ⁻¹ x 10 ⁻⁶)	46	12	40	12
	B_i (m.s ⁻¹ x 10 ⁻⁶)	0.33	0.23	0.41	0.22
	k_i/B_i	139	52	98	55
ESPA4	k_i (m.s ⁻¹ x 10 ⁻⁶)	23	42	18	40
	B_i (m.s ⁻¹ x 10 ⁻⁶)	0.05	0.10	0.05	0.09
	k_i/B_i	460	420	360	444

452

453 **Table 11**

454 B_i for glucose deduced from several publications obtained with the simplified Solution-Diffusion model
 455 taking [concentration polarization](#) into account (eq. 9)

Reference		Nguyen, N. et al., 2016	Almazán et al., 2015	Lyu et al., 2016		Mohammad et al., 2010	Wang et al., 2018	Zhou et al., 2013a, b
$C_{glucose}$ (g.L ⁻¹)		10	5-100	20	0.5	3-12	4-20	4-20
DK	B_i (m.s ⁻¹ x 10 ⁻⁶)	0.27	0.95	0.54	0.25	0.37	0.91	0.59

456

457 5. Conclusion

458 A complex cauliflower processing wastewater resulting from blanching was treated using membrane
459 processes, in order to produce water of a quality high enough to be reused inside the factory. The adopted
460 pre-treatment consisted in a double sieving step at 169 μm and 79 μm followed by a 100 000 $\text{g}\cdot\text{mol}^{-1}$ MWCO
461 ultrafiltration. Its removal efficiency reached 99% for turbidity, 50% for COD and 40% for conductivity
462 especially. At industrial scale, this pre-treatment could be replaced by a single submerged hollow fibre
463 ultrafiltration (Nelson et al., 2007). RO treatment with ESPA4 membrane was then necessary to reach the
464 best permeate quality. It was optimized at 19 bar, leading to a residual COD value in the permeate of 225
465 $\text{mg O}_2\cdot\text{L}^{-1}$ due to the transfer of small non-aromatic compounds. Solution-Diffusion model and film model
466 theory were applicable to describe glucose and fructose transfer, for DK, NF270 and ESPA4 membranes.
467 Permeability coefficient B_i obtained for glucose and fructose was similar ($0.45 \times 10^{-6} \text{ m}\cdot\text{s}^{-1}$) and consistent
468 with values calculated from other studies (0.25 to $0.95 \times 10^{-6} \text{ m}\cdot\text{s}^{-1}$) regardless of the concentration of glucose
469 in the feed solution and its composition.

470 These results, if industrially confirmed, open the possibility of water recycling of cauliflower blanching
471 wastewater. However, it would be necessary to investigate long-term accumulation of the residual solutes in
472 the recycled effluent. A Life Cycle Assessment on the plant under study confirmed that this wastewater
473 recycling through UF plus RO treatment was beneficial. It offers a way to limit the reliance on water
474 resource and to face water restrictions that in certain regions lead to stop or delay food plants production.

475

476 Nomenclature and units

477	A_w	membrane permeability to pure water ($\text{m}\cdot\text{s}^{-1}\cdot\text{Pa}^{-1}$ or $\text{L}\cdot\text{h}^{-1}\cdot\text{m}^2\cdot\text{bar}^{-1}$)
478	B_i	membrane permeability to solute i ($\text{m}\cdot\text{s}^{-1}$)
479	$C_{p,i}, C_{r,i}, C_{r m,i}$	concentration of solute i in the permeate, the retentate and at the membrane interface in the 480 retentate, respectively ($\text{mol}\cdot\text{m}^{-3}$)
481	CH	Carbonate Hardness ($^\circ\text{f}$)
482	COD	Carbon Oxygen Demand ($\text{mg O}_2\cdot\text{L}^{-1}$)
483	COD_{diff}	differential COD = difference between COD and $\text{COD}_{\text{sugars}}$
484	$\text{COD}_{\text{sugars}}$	COD deduced from sugar concentrations ($\text{mg O}_2\cdot\text{L}^{-1}$)
485	$\Delta\pi$	osmotic pressure gradient between the membrane interface in the retentate and the permeate 486 (Pa or bar)
487	J_i	flux of solute i through the membrane ($\text{mol}\cdot\text{s}^{-1}\cdot\text{m}^{-2}$)
488	J_p	permeate flux ($\text{m}\cdot\text{s}^{-1}$, usually expressed in $\text{L}\cdot\text{h}^{-1}\cdot\text{m}^{-2}$)

489	k_i	mass transfer coefficient of solute i in the polarization layer ($\text{m}\cdot\text{s}^{-1}$)
490	OD	Optical Density (-)
491	P_f, P_r, P_p	pressure in the feed, the retentate and the permeate, respectively (Pa or bar)
492	$\pi_p, \pi_{r m}$	osmotic pressure in the permeate and at the membrane interface in the retentate, respectively
493		(Pa or bar)
494	Q_p	permeate flow rate ($\text{m}^3\cdot\text{s}^{-1}$ or $\text{L}\cdot\text{h}^{-1}$)
495	S	effective membrane area (m^2)
496	TMP	TransMembrane Pressure (Pa or bar)
497	TN	Total Nitrogen ($\text{mg N}\cdot\text{L}^{-1}$)
498	Tr_i	rejection rate of solute i (-)
499	TSS	Total Suspended Solids ($\text{mg}\cdot\text{L}^{-1}$)
500	V_i, V_f	initial and final volume of solution in the feed tank for a discontinuous filtration run (m^3)
501	VRR	Volume Reduction Ratio (-)

502 **Acknowledgements**

503 This research was supported by the French National Agency for Research (ANR) through the MINIMEAU
504 Project (ANR-17-CE10-0015). Authors thank Janaina Oliveira da Silva for her valuable contribution to this
505 work. Technical Center for Food Product Conservation (CTCPA, Paris, France) is acknowledged for sharing
506 its expertise in vegetable industries and for providing the industrial partner for effluent supply.

507

508 **References**

- 509 Aimar, P. (2006). Filtration membranaire (OI, NF, UF) Mise en œuvre et performances. *Techniques de*
510 *l'ingénieur Procédés de traitement des eaux potables, industrielles et urbaines* base documentaire :
511 TIB318DUO(ref. article : w4110).
- 512 Aimar, P., Bacchin, P., & Maurel, A. (2010). Filtration membranaire (OI, NF, UF, MFT) Aspects
513 théoriques : perméabilité et sélectivité. *Techniques de l'ingénieur Opérations unitaires : techniques*
514 *séparatives sur membranes* base documentaire : TIB331DUO(ref. article : j2790).
- 515 Almazán, J.E., Romero-Dondiz, E.M., Rajal, V.B., & Castro-Vidaurre, E.F. (2015). Nanofiltration of
516 glucose: Analysis of parameters and membrane characterization. *Chemical engineering research and*
517 *design* 94, 485-493.
- 518 Bhandari, S.R., & Kwak, J.-H. (2015). Chemical composition and antioxidant activity in different tissues of
519 Brassica vegetables. *Molecules* 20(1), 1228-1243.
- 520 Bortoluzzi, A.C., Faitão, J.A., Di Luccio, M., Dallago, R.M., Steffens, J., Zobot, G.L., & Tres, M.V. (2017).
521 Dairy wastewater treatment using integrated membrane systems. *Journal of environmental chemical*
522 *engineering* 5(5), 4819-4827.
- 523 Braeken, L., Van der Bruggen, B., & Vandecasteele, C. (2004). Regeneration of brewery waste water using
524 nanofiltration. *Water Research* 38(13), 3075-3082. [https://doi.org/ 10.1016/j.watres.2004.03.028](https://doi.org/10.1016/j.watres.2004.03.028).
- 525 Brião, V.B., Salla, A.C.V., Miorando, T., Hemkemeier, M., & Favaretto, D.P.C. (2019). Water recovery
526 from dairy rinse water by reverse osmosis: Giving value to water and milk solids. *Resources,*
527 *Conservation and Recycling* 140, 313-323.
- 528 Casani, S., Rouhany, M., & Knochel, S. (2005). A discussion paper on challenges and limitations to water
529 reuse and hygiene in the food industry. *Water Research* 39(6), 1134-1146. [https://doi.org/](https://doi.org/10.1016/j.watres.2004.12.015)
530 [10.1016/j.watres.2004.12.015](https://doi.org/10.1016/j.watres.2004.12.015).
- 531 Dewettinck, K., & Le, T.T. (2011). *Membrane separations in food processing*. Cambridge, The Royal
532 Society of Chemistry.
- 533 Epsztein, R., Shaulsky, E., Dizge, N., Warsinger, D.M., & Elimelech, M. (2018). Role of ionic charge
534 density in donnan exclusion of monovalent anions by nanofiltration. *Environmental science & technology*
535 *52(7)*, 4108-4116.
- 536 European, C. (2018). *Best Available Technique (BAT) - Reference document in the food, drink and milk*
537 *industries*.
- 538 Freger, V. (2003). Nanoscale heterogeneity of polyamide membranes formed by interfacial polymerization.
539 *Langmuir* 19(11), 4791-4797.
- 540 Garnier, C., Guiga, W., Lameloise, M.-L., Degrand, L., & Fargues, C., 2019. Tools development for water
541 recycling. 9th IWA Membrane Technology Conference (Toulouse), Poster.
- 542 Garnier, C., Guiga, W., Lameloise, M.-L., Degrand, L., & Fargues, C. (2020). Toward the reduction of water
543 consumption in the vegetable-processing industry through membrane technology: case study of a carrot-
544 processing plant. *Environmental Science and Pollution Research*, 1-19.

545 Guiga, W., & Lameloise, M.-L. (2019). Membrane separation in food processing. *Green Food Processing*
546 *Techniques* (pp. 245-287). Elsevier.

547 [Lide, D.R. \(2004\). *CRC handbook of chemistry and physics*. CRC press.](#)

548 Lyu, H., Fang, Y., Ren, S., Chen, K., Luo, G., Zhang, S., & Chen, J. (2016). Monophenols separation from
549 monosaccharides and acids by two-stage nanofiltration and reverse osmosis in hydrothermal liquefaction
550 hydrolysates. *Journal of Membrane Science* 504, 141-152.

551 Meneses, Y.E., Stratton, J., & Flores, R.A. (2017). Water reconditioning and reuse in the food processing
552 industry: Current situation and challenges. *Trends in Food Science & Technology* 61, 72-79.
553 <https://doi.org/10.1016/j.tifs.2016.12.008>.

554 Mohammad, A.W., Basha, R.K., & Leo, C. (2010). Nanofiltration of glucose solution containing salts:
555 Effects of membrane characteristics, organic component and salts on retention. *Journal of Food*
556 *Engineering* 97(4), 510-518.

557 Nelson, H., Singh, R., Toledo, R., & Singh, N. (2007). The use of a submerged microfiltration system for
558 regeneration and reuse of wastewater in a fresh-cut vegetable operation. *Separation Science and*
559 *Technology* 42(11), 2473-2481. <https://doi.org/10.1080/01496390701477147>.

560 Nguyen, D., Lameloise, M.-L., Guiga, W., Lewandowski, R., Bouix, M., & Fargues, C. (2016). Optimization
561 and modeling of nanofiltration process for the detoxification of ligno-cellulosic hydrolysates-study at
562 pre-industrial scale. *Journal of Membrane Science* 512, 111-121.

563 Nguyen, N., Fargues, C., Guiga, W., & Lameloise, M.-L. (2015). Assessing nanofiltration and reverse
564 osmosis for the detoxification of lignocellulosic hydrolysates. *Journal of Membrane Science* 487, 40-50.

565 Nguyen, N., Lameloise, M.-L., Guiga, W., Lewandowski, R., Bouix, M., & Fargues, C. (2016). Optimization
566 and modeling of nanofiltration process for the detoxification of ligno-cellulosic hydrolysates-study at
567 pre-industrial scale. *Journal of Membrane Science* 512, 111-121.

568 Paramithiotis, S., Hondrodinou, O.L., & Drosinos, E.H. (2010). Development of the microbial community
569 during spontaneous cauliflower fermentation. *Food Research International* 43(4), 1098-1103.

570 Qasim, M., Badrelzaman, M., Darwish, N.N., Darwish, N.A., & Hilal, N. (2019). Reverse osmosis
571 desalination: A state-of-the-art review. *Desalination* 459, 59-104.

572 [Shannon, R.D. \(1976\). Revised effective ionic radii and systematic studies of interatomic distances in halides
573 and chalcogenides. *Acta crystallographica section A: crystal physics, diffraction, theoretical and general*
574 *crystallography* 32\(5\), 751-767.](#)

575 Sim, L.N., Chong, T.H., Taheri, A.H., Sim, S., Lai, L., Krantz, W.B., & Fane, A.G. (2018). A review of
576 fouling indices and monitoring techniques for reverse osmosis. *Desalination* 434, 169-188.

577 Suárez, A., Fidalgo, T., & Riera, F.A. (2014). Recovery of dairy industry wastewaters by reverse osmosis.
578 Production of boiler water. *Separation and Purification Technology* 133, 204-211. <https://doi.org/10.1016/j.seppur.2014.06.041>.

579

580 Wang, T., Meng, Y., Qin, Y., Feng, W., & Wang, C. (2018). Removal of furfural and HMF from
581 monosaccharides by nanofiltration and reverse osmosis membranes. *Journal of the Energy Institute* 91(3),
582 473-480.

583 Warsinger, D.M., Chakraborty, S., Tow, E.W., Plumlee, M.H., Bellona, C., Loutatidou, S., Karimi, L.,
584 Mikelonis, A.M., Achilli, A., & Ghassemi, A. (2018). A review of polymeric membranes and processes
585 for potable water reuse. *Progress in polymer science* 81, 209-237.

586 Wenten, I.G., & Khoiruddin (2016). Reverse osmosis applications: Prospect and challenges. *Desalination*
587 391, 112-125. [https://doi.org/ 10.1016/j.desal.2015.12.011](https://doi.org/10.1016/j.desal.2015.12.011).

588 Wijmans, J.G., & Baker, R.W. (1995). The solution-diffusion model: a review. *Journal of membrane science*
589 107(1-2), 1-21.

590 Zhou, F., Wang, C., & Wei, J. (2013a). Separation of acetic acid from monosaccharides by NF and RO
591 membranes: Performance comparison. *Journal of membrane science* 429, 243-251.

592 Zhou, F., Wang, C., & Wei, J. (2013b). Simultaneous acetic acid separation and monosaccharide
593 concentration by reverse osmosis. *Bioresource technology* 131, 349-356.

594